J. Membrane Biol. 49, 363–390 (1979)

On the Cross-Reactivity of Amiloride and 2,4,6 Triaminopyrimidine (TAP) for the Cellular Entry and Tight Junctional Cation Permeation Pathways in Epithelia

R.S. Balaban, L.J. Mandel, and D.J. Benos*

Department of Physiology, Duke University, Durham, North Carolina 27710

Received 20 March 1979; revised 25 May 1979

Summary. 2,4,6 Triaminopyrimidine (TAP) has been previously shown to inhibit the passive tight junctional cation permeation pathway in various "leaky" epithelia. Amiloride has been shown to be an effective inhibitor of the cation cellular entry pathway in "tight" epithelia. In this paper we demonstrate that TAP and amiloride at appropriate concentrations are able to block either of these epithelial cation permeation pathways. TAP was found to block the Na entry pathway in frog skin with the following characteristics: it (1) inhibits from the external solution only, (2) is completely reversible, (3) increases the transepithelial resistance, (4) is active in the monoprotonated form, (5) is noncompetitive with Na, (6) displays saturation kinetics which obey a simple kinetic model ($K_I = 1 \times 10^{-3}$ M), (7) is independent of external calcium, (8) is dependent on external buffering capacity, and (9) is competitive with amiloride. Amiloride inhibition of the junctional permeation in gallbladder had the following characteristics: it (1) increases the transepithelial resistance, (2) decreases cation conductance without affecting the anion conductance, (3) displays saturation kinetics which obey a simple kinetic model ($K_I = 1 \times 10^{-3}$ M), and (4) possesses inhibitory activity in both its protonated and unprotonated form. These results not only indicate that a similar inhibitory site may exist in both of these cation permeation pathways, but also provide information on the chemical nature and possible location of these inhibitory sites.

Two main pathways for cationic permeation have been identified across epithelial tissues, the transcellular and the extracellular. Cations which permeate an epithelium via the extracellular pathway are believed to traverse through the tight junctions between adjacent epithelial cells. This results in the passive transepithelial movement of ions without the

* *Present address:* Department of Physiology and Laboratory of Human Reproduction and Reproductive Biology, Harvard Medical School, Boston, Massachusetts 02115.

0022-2631/79/0049-0363 $05.60

necessity for ion entry into epithelial cells. The low electrical resistance found in most "leaky" epithelia (i.e., transepithelial resistance $<300\,\Omega\,cm^2$) has been shown to be due to the low resistance of this extracellular pathway (Fromter & Diamond, 1972). Examples of leaky epithelial include gallbladder, duodenum, and renal proximal tubule.

The transcellular pathway may be described in terms of two steps: cation entry through the apical membrane followed by cellular extrusion across the basolateral membrane. In numerous epithelia the entry step, or cellular entry pathway, appears to be passive, whereas the cellular extrusion at the basolateral membrane is an active process mediated by ion pumps. In the frog skin, several lines of evidence indicate that the movement of Na through the cellular entry pathway is the rate-limiting step in the active transcellular movement of Na in this epithelium (*see* Mandel (1978) for discussion). The cellular entry pathway has been extensively studied in so-called "tight" epithelia (transepithelial resistance $>300\,\Omega\,cm^2$). These epithelia can form and/or maintain large ionic or osmotic gradients and possess a very high tight junctional pathway electrical resistance (Diamond, 1978). Examples of tight epithelia include frog skin, colon, and renal collecting duct.

Both the junctional and the cellular cation permeation pathways have been the subject of comprehensive studies designed to unravel their chemical and physical properties (Moreno & Diamond, 1975*a*; Lindemann & Voute, 1976; Diamond, 1978). Particular problems that have been investigated relate to the ionic permeation and selectivity, as well as the specific roles each of these pathways plays in the movement of ions and water across epithelia. One method of studying these pathways has been the use of specific inhibitors to probe the sites under various physiological conditions (Diamond, 1978; Cuthbert, 1977; Cuthbert & Shum, 1976; Benos *et al.*, 1976; Moreno, 1975) and to eliminate specific permeation pathways for various experimental and medical purposes. Two inhibitors have been extensively used in these studies: 2,4,6 triaminopyrimidine (TAP) on the tight junctional permeation pathway of leaky epithelia (Moreno, 1975), and amiloride on the cellular entry pathway of tight epithelia (Salako & Smith, 1970; Biber, 1971).

This study represents a kinetic description of the cross-reactivity of these inhibitors, TAP and amiloride, on the two epithelial cation permeation pathways. Two preparations were utilized in this investigation: (i) the frog skin, a tight epithelium, for the cellular entry pathway, and (ii) the frog gallbladder, a leaky epithelium, for the tight junctional pathway. These experiments were performed not only to clarify the effects of these

popular inhibitors but also to determine if any pharmacological similarities exist between these two epithelial cation selective permeation pathways.

Materials and Methods

Bullfrog Skin Preparation

The abdominal skins of bullfrogs *(Rana catesbeiana)* were mounted as flat sheets (3.14 cm^2 in area) between Lucite chambers equipped with solution reservoirs similar to those described by Schultz and Zalusky (1964).

The open circuit potential across the skin was measured with calomel electrodes, and current was passed through the skin via Ag/AgCl electrodes. Both pairs of electrodes were connected to the solution reservoirs with agar bridges having a composition of the standard Ringer plus 4 % agar. An automatic voltage clamp that compensated for the resistance of the solution between the agar bridges was used to pass the appropriate current through the skin to clamp the membrane potential at zero millivolts. This current, defined as the short-circuit current (I_{sc}) was utilized as a measure of the active outside to inside net flux of Na ions as previously demonstrated by Ussing and Zerahn (1951) and by ^{22}Na flux experiments conducted under some conditions of this investigation. ^{22}Na influx experiments were performed by methods previously described (Mandel & Curran, 1973).

The transepithelial resistance was calculated, using Ohm's law, from the voltage deflections produced in response to constant current pulses delivered across an open circuited skin from a constant current generator (Nuclear Chicago, Model 7510). The chamber and specific solution resistances were compensated by measuring the voltage deflection in the absence of the skin and subtracting this voltage from that obtained in the presence of the skin. The composition of the standard Ringer solution used for this preparation, unless specified differently, was (in mmol/liter): NaCl, 85; $CaCl_2$, 1; KCl, 5; $NaHCO_3$, 25; and glucose, 2, mixed and aerated with a 95 % O_2/5 % CO_2 gas mixture to obtain a solution pH of 7.4 at room temperature.

Calcium-free outer solutions were obtained by first washing the external chamber with a Ringer solution containing no Ca and 1 mM ethyleneglycol bis (6-aminoethylether)-N, N-tetraacetic acid (EGTA) followed by replacement of the EGTA solution with Ca-free Ringer without EGTA.

Due to the variability usually encountered from skin to skin, care was taken to perform each group of experiments on the same shipment of frogs; in addition, whenever possible, each skin served as its own control to aid in validating any changes observed.

Bullfrog Gallbladder Preparation

Gallbladders were excised from decapitated bullfrogs, washed free of bile with Ringer, and mounted in an Ussing-type chamber (Cala, Cogswell & Mandel, 1978) with Sylgard washers to limit edge damage (cross sectional area 2.7 cm^2). Transepithelial potential differences (PD) and resistances were measured as described for the frog skin. The current bridges were 15.0 mm, while the voltage recording bridges were 1.5 mm from the eipthelium. The standard Ringer for this preparation had the following composition (in mmol/liter): NaCl, 150; $CaCl_2$, 0.25; KH_2PO_4, 4; HEPES, 3; pH 7.0.

Bladders were allowed to equilibrate for 60 to 90 min at room temperature. Bladders displaying sodium dilution potentials (*see* below) less than 9 mV or spontaneous potentials greater than 2 mV with identical solutions on both sides were discarded.

The method of determining sodium (G_{Na}) and chloride (G_{Cl}) conductances was that of Moreno and Diamond (1974). Briefly, NaCl dilution potentials were measured by replacing half of the NaCl in the mucosal solution isosmotically with mannitol. These potentials were corrected for electrode junction potentials as described by Barry and Diamond (1970). Permeability ratios for Na and Cl were then calculated from the measured dilution potentials using the Goldman-Hodgkin-Katz equation with the appropriate activity coefficients (Robinson & Stokes, 1970). In gallbladder, the Na to Cl permeability ratio has been shown to equal to the ratio of the ionic conductances of these species (Barry, Diamond & Wright, 1971; Barry & Diamond, 1971). Utilizing this permeability ratio, G_{Cl} may be calculated from the following equation:

$$G_{Cl}=\frac{G_T}{1+(P_{Na}/P_{Cl})} \tag{1}$$

where G_T = total tissue conductance and P_{Na}/P_{Cl} = the Na to Cl permeability ratio as calculated from the Goldman equation.

The permeation pathway for Cl in the gallbladder epithelium has been attributed to a damage or leakage pathway. Some Na is also assumed to move through this leakage pathway in such a way that the ratio of Na to Cl transport numbers equals their free solution mobility ratio (i.e., μ_{Na}/μ_{Cl}) (Barry *et al.*, 1971; Moreno & Diamond 1974, 1975*a*, *b*). Using this assumption, the total conductance of this leakage pathway can be calculated from the following equation:

$$G_{leak}=\text{leakage conductance}=G_{Cl}(1+\mu_{Na}/\mu_{Cl}). \tag{2}$$

Thus, the value used for the Na conductance of the tissue corrected for the shunt pathway conductance was calculated from the following equation:

$$G_{Na}=G_T-G_{Cl}(1+\mu_{Na}/\mu_{Cl}). \tag{3}$$

The exclusion of K permeabilities in Eqs. (1)–(3) in the calculation of G_{Na} and G_{Cl} for frog gallbladder results in an error of less than 3 % (Moreno, 1975).

2, 4, 6 Triaminopyrimidine was obtained from Sigma Chemical Company, St. Louis, Missouri. Amiloride was a gift from Merck Sharp & Dohme Research Laboratories, West Point, Pa. Since amiloride is prepared as the HCl, the excess Cl was compensated for when amiloride was added to one side of the bladder. All calculations and modeling were performed on a PDP 8E digital computer. Where applicable, all values are expressed as the mean ± one SEM.

Results

TAP Inhibition of the Na Entry Pathway in Frog Skin

A. Site of Action and Kinetics of Inhibition

As shown in Fig. 1, 10 mM TAP added to the inside solution had no effect on the I_{sc}; however, addition of 10 mM TAP to the outside solution

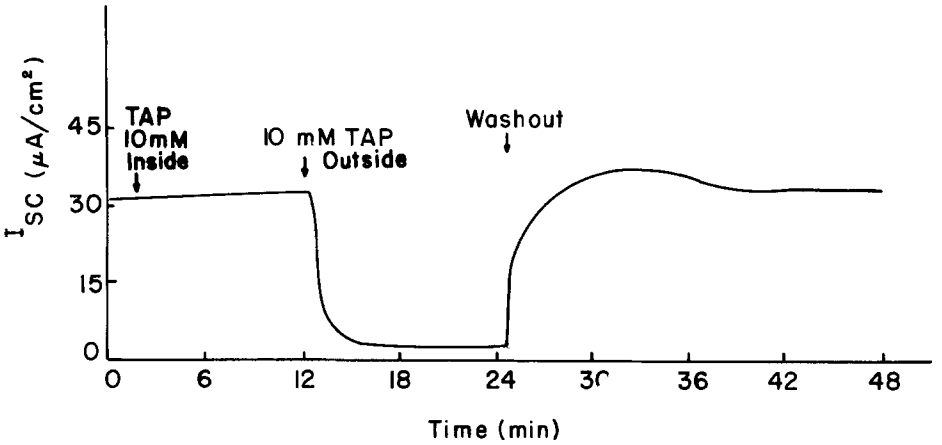

Fig. 1. Effect of 10 mM TAP in the internal or external solutions on the I_{sc} of the isolated frog skin as a function of time. This tracing is from one representative experiment

elicited a rapid inhibition of I_{sc}. This inhibition by TAP was rapidly reversed by washing the external chamber with TAP-free Ringer (Fig. 1). These results suggested that TAP acted by inhibiting the rate-limiting Na entry pathway at the apical membrane, since TAP was only effective from the outside solution. This possibility was investigated further by studying the effects of TAP on the transepithelial resistance.

It has been shown that 75 to 95 % of the transepithelial resistance of the frog skin occurs across the apical membrane (Helman & Fisher, 1977). Furthermore, the majority of this membrane's conductance is due to Na permeation through the cellular entry pathway. Thus, the transepithelial resistance would be expected to increase if TAP were to inhibit the cellular entry pathway. The effect of TAP on the transepithelial resistance of the frog was investigated using an open circuited frog skin, across which hyperpolarizing constant current pulses were passed (*see* Methods). Figure 2 illustrates that a dose-dependent increase in transepithelial resistance was observed with the addition of 1.25 and 5 mM TAP to the outside solution. The height of the shaded area represents the magnitude of the positive voltage deflection in response to a 50 μA current pulse. 5.0 mM TAP resulted in a 66 ± 4.0 % increase in the resistance of 5 skins; this increased resistance was completely reversed upon washing with drug-free Ringer. These results support the notion that TAP acts by inhibiting the apical entry of Na in this epithelium.

The dose-response characteristics of TAP as an inhibitor of I_{sc} were investigated by progressively adding higher concentrations of TAP to the

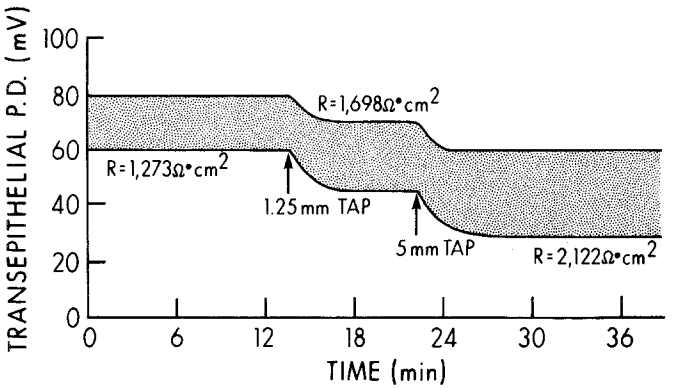

Fig. 2. Effect of 1.25 and 5 mM TAP on the transepithelial resistance of the isolated frog skin as a function of time. Transepithelial resistance was calculated from the voltage deflection (upper line on graph) in response to a hyperpolarizing transepithelial current pulse. The lower line represents the baseline transepithelial potential

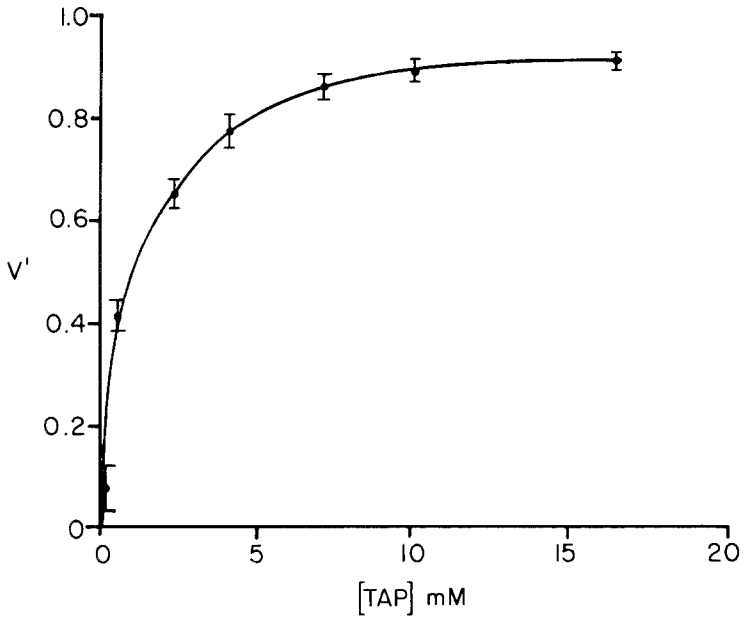

Fig. 3. TAP dose-response inhibition of the I_{sc} in the frog skin. Additions were made to the external solution. The results are presented as fractional inhibition (V') as a function of the external TAP concentration. Data points are the mean of 25 experiments, and the bars indicate 1 SEM

outside solution (Fig. 3). Because of the variable I_{sc} baselines found in different skins, the inhibitory effect of TAP was expressed as the fractional inhibition (V') of I_{sc} produced by a given TAP concentration:

$$V' = 1 - \frac{I_{TAP}}{I_{sc}} \tag{4}$$

where I_{TAP} is the I_{sc} in the presence of a given concentration of TAP. The inhibitory affinity of TAP, (K_I or, specifically, K_{TAP}), defined as the concentration of TAP necessary to produce a 50 % inhibition of I_{sc}, was estimated to be 1 mM from this curve.

The kinetic properties of TAP inhibition of I_{sc} were investigated further under the assumption that the rate of Na transport as a function of external Na concentrations was described by Michaelis-Menten kinetics. This type of analysis was based on two major assumptions: (i) the movement of Na through the apical cellular entry pathway is rate limiting for the transepithelial movement of Na, and (ii) the interaction of Na at the apical membrane entry pathway is with a fixed number of sites and is completely reversible. The evidence supporting these assumptions and a complete discussion of the application of Michaelis-Menten kinetics to Na transport in the frog skin is available in other publications from this laboratory (Mandel, 1978; Benos, Mandel & Balaban, 1979). This treatment allows the investigation of several characteristics of the inhibition of Na transport by TAP. The first of these involves the determination of whether this inhibition of I_{sc} is competitive or noncompetitive with sodium at the cellular entry pathway. To this end, experiments were performed to examine the effect of external sodium concentration on TAP inhibition. If TAP were competitive with Na, a decrease in K_{TAP} with decreasing Na concentration would be expected. In contrast, if TAP were noncompetitive with Na, K_{TAP} should remain constant with changes in external Na concentration (Benos *et al.*, 1979). As seen in Fig. 4, where V' is plotted as a function of log [TAP], K_{TAP} did not significantly change with variations in external Na. This behavior indicates that TAP interacts with the Na entry site in a noncompetitive manner.

Utilizing the Michaelis-Menten treatment further, we proceeded to determine whether TAP's interaction with Na followed a simple noncompetitive model. An equation for noncompetitive inhibition of Na transport may be derived using a Michaelis-Menten equation for both Na and TAP's interaction at their respective sites [*see Appendix;* Eq. (A3)].

$$V' = 1 - \frac{V' K_{TAP}}{[TAP]}. \tag{5}$$

To conform with this model, a single reciprocal plot of V' *vs.* $V'/[TAP]$

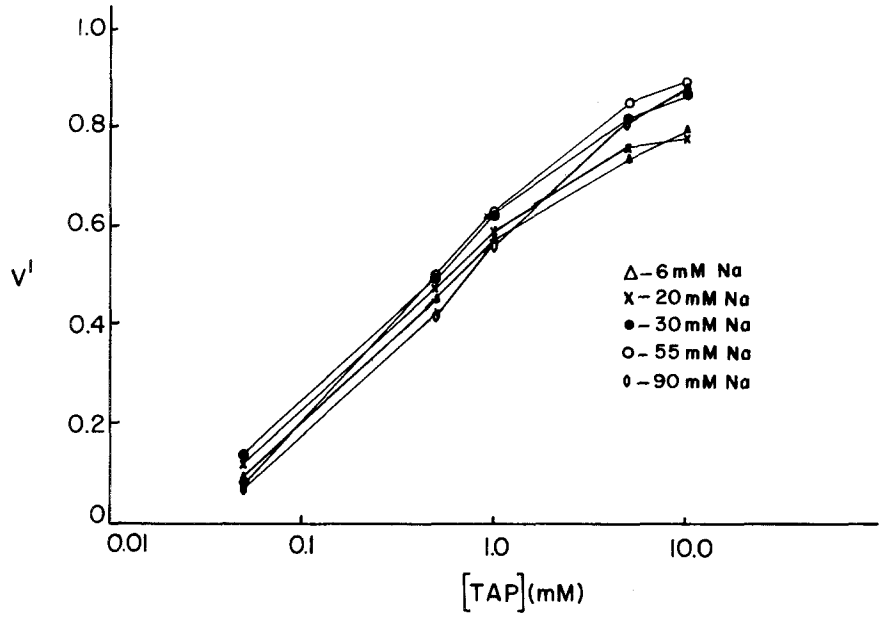

Fig. 4. Log-dose response curves of fractional TAP inhibition of $I_{sc}(V')$ of frog skin at sodium concentrations of 90, 55, 30, 20, and 6 mM. An osmotically equivalent amount of choline chloride was used to replace NaCl on both sides. Each point represents the mean value of twelve experiments. TAP concentrations were chosen to magnify any changes in the 50 % inhibition (K_{TAP}) region for TAP. The SE bars were omitted for clarity

should be linear with a slope equal to negative K_{TAP} and an ordinate intercept equal to 1 (corresponding to 100 % inhibition). It was found that individual TAP dose-response experiments resulted in linear plots with a mean correlation coefficient of 0.96 (± 0.01) in 25 skins. However, K_{TAP} of individual experiments was found to be highly variable ranging from 0.6 to 3.6 mM (mean value $= 1.65 \pm 0.17$ mM) with the extrapolated maximal inhibition by TAP also varying from 86 % to 100 % (mean $= 95 \pm 0.1$ %). Figure 5 illustrates an example of a single reciprocal plot of the mean TAP dose-response data obtained from four skins from the same frog. K_{TAP} was 1.0 mM, and the maximal inhibition extrapolated from the regression line ($r^2 = 0.99$) was 100 % (or $V' = 1.0$) in these particular skins. From these data, it appears that the inhibition of Na transport by TAP in frog skin may be described by a simple Michaelis-Menten noncompetitive kinetic scheme. In some cases, up to 14 % of the measured I_{sc} was insensitive to TAP inhibition; however, high linear correlation coefficients were still obtained from the dose-response data, indicating that the TAP-sensitive I_{sc} still obeyed this Michaelis-Menten model.

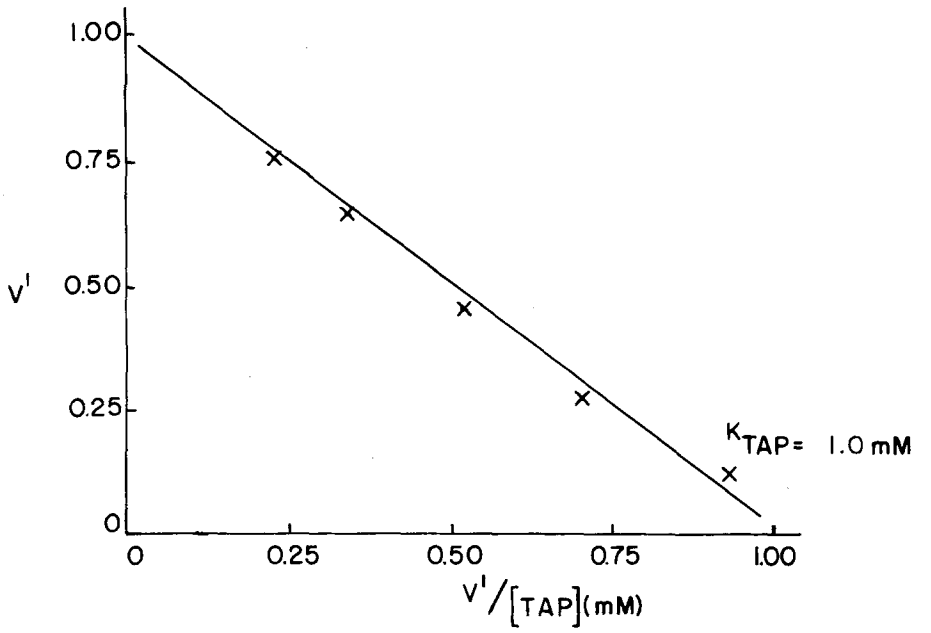

Fig. 5. Single reciprocal plot of TAP fractional inhibition of I_{sc} (V') *vs.* TAP fractional inhibition divided by the TAP concentration in the external medium (V'/[TAP]). Points represent the mean of four paired experiments from the skin of one frog. The regression line through the data points has a correlation coefficient of >0.99

The good correlation between the TAP dose-response data points with this Michaelis-Menten kinetic model suggests that TAP interacts with its site in a simple one-to-one manner with little or no cooperativity between inhibitory sites. Additional support for this hypothesis was obtained by replotting TAP dose-response data in a noncompetitive Hill plot (Benos *et al.*, 1979) and calculating a Hill coefficient of 0.91 ± 0.06 ($n = 6$), which is not significantly different from one. A Hill coefficient of one indicates that the stoichiometry of TAP with its site is one-to-one and that little or no cooperativity occurs between inhibitory sites.

B. Effects of pH and Buffering Capacity

In initial experiments, it was found that TAP was relatively ineffective as an inhibitor of I_{sc}, ($K_{TAP} > 5$ mM), when the frog skin was bathed in the commonly used Ringer solution containing 2.5 mM HCO_3 which, when bubbled with room air, has a pH of 8.4. This lack of inhibition occurred even when the pH of the solution was adjusted to 7.4

Table 1. Na^{22} influxes compared to measured I_{sc} in low and high bicarbonate Ringer solutions

Bathing solution[b]	Sodium influx[a, c]	Short-circuit current[a, c]
	($\mu A/cm^2$)	($\mu A/cm^2$)
2.5 mM HCO_3	26.3 ± 2.3	22.8 ± 2.9
25.0 mM HCO_3	8.3 ± 1.2	9.9 ± 1.4

[a] $n=8$.
[b] pH constant at 7.4.
[c] Errors given are ±SEM.

with CO_2. However, in 25 mM HCO_3 Ringer bubbled with 95 % O_2/5 % CO_2 (pH 7.4), TAP was highly effective in inhibiting the I_{sc}, as shown earlier. In an attempt to explain this puzzling result, investigations were pursued to determine if the I_{sc} still measured active Na influx in the 25 mM HCO_3 buffer solution and the effect of buffering capacity on the inhibitory action of TAP. In accordance with the first of these goals, ^{22}Na influx experiments were conducted under short-circuit conditions in 25 mM HCO_3 solutions. These data are presented in Table 1 and are compared to ^{22}Na influxes obtained in the same skins bathed with 2.5 mM HCO_3 solutions. Both sets of experiments were conducted at pH 7.4 by adjusting the CO_2 concentration. From these data, it is evident that, within experimental variability, the I_{sc} accurately represented the active Na influx in both the high and low bicarbonate solutions. An unexpected result was that the I_{sc} observed in 25 mM HCO_3 was ony 44 % of that measured in 2.5 mM HCO_3. We, therefore, decided to investigate the kinetics of HCO_3/CO_2 inhibition of I_{sc} because of its potential in clarifying the mechanism of HCO_3/CO_2 augmentation of TAP's potency. Experiments were performed to determine the effects of bicarbonate on the apparent Michaelis-Menten affinity constant for Na (K_{Na}) and the maximum I_{sc} (I_{max}). Following the methods of Mandel (1978), I_{sc} was measured as a function of various external Na concentrations and, thereafter, I_{max} and K_{Na} were calculated using the Michaelis-Menten rate equation. Two bicarbonate buffer concentrations were used, 25 and 2.5 mM, in 7 skins gassed with appropriate amounts of CO_2 to obtain a stable pH of 7.4. It was found that K_{Na} was not significantly affected by the HCO_3 concentrations; 17.0 ± 0.7 mM in 25 mM HCO_3 and 16.9 ± 0.7 mM in 2.5 mM HCO_3. In contrast, I_{max} with 25 mM HCO_3 was inhibited 49.3 ± 1.3 % with respect to 2.5 mM HCO_3. Apparently, the effect of 25 mM HCO_3 is to decrease the I_{max} of the Na transport process without affecting the K_{Na}.

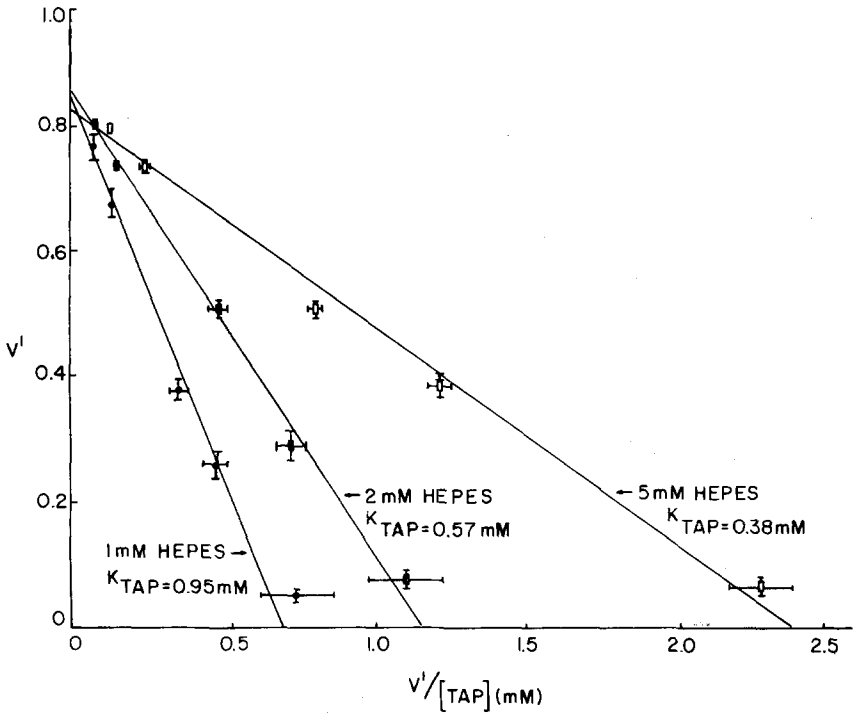

Fig. 6. Single reciprocal plot of V' *vs.* $V'/[TAP]$ in the isolated bullfrog skin at external HEPES concentrations of 1, 2 and 5 mM. The pH was maintained constant at 7.4. Data points represent the mean of 7 experiments, bars indicate 1 SEM. K_{TAP} was obtained from the slopes of the regression lines of these data; in all cases the r^2 was >0.97

Next, experiments were performed using the organic buffer HEPES to test the effect of buffering capacity on the potency of TAP. This organic buffer was used so that different buffering capacities of the bathing solution could be easily obtained by varying the HEPES concentration without altering the bulk pH. TAP dose response experiments were conducted in external and internal Ringer solutions buffered with 1, 2, and 5 mM HEPES at a constant pH of 7.4. $NaHCO_3$ was omitted from these HEPES-buffered solutions and was replaced with NaCl. The external solution was gassed and mixed with 100% O_2. HEPES concentrations of less than 1 mM in the external solution resulted in an unstable pH, with the pH slowly becoming more acidic. Figure 6 shows these experimental data plotted in a single reciprocal form (Eq. (5)) to obtain accurate values for K_{TAP} and the maximal inhibition by TAP. A decrease in K_{TAP} was observed with increasing buffering capacity (or concentration of HEPES), that is, $K_{TAP}=0.38$ at 5 mM; 0.57 at 2 mM; and 0.95 at 1 mM, without any change in the maximal inhibition by the drug.

These experiments demonstrate that the buffering capacity of the external solution has a direct action on the inhibitory potency of TAP at pH 7.4. Several experiments performed at pH 6.0 with other organic buffers (cacodylate and MES) demonstrated that the potency of TAP was independent of buffering capacity at this pH. The concentration of bicarbonate and HEPES buffers were found to have no demonstrable effect on the inhibitory action of amiloride at pH 7.4.

TAP can exist in one of three forms: an uncharged form at high pH, a mono-cation at near neutral pH ($pK_a = 6.74$) and as a di-cation in the stong acid region ($pK_a = 1.31$) (Roth & Stelitz, 1969). In order to identify which of these species of the TAP molecule is active, we investigated the effect of external bath pH on the potency of the TAP molecule. Due to the aforementioned dependence of TAP inhibition on buffering capacity, a specially buffered external solution was used in these experiments to produce a uniform buffering capacity at the external pH values we examined. The buffered Ringer was composed of the standard Ringer solution with HCO_3 replaced by the following buffers (mM) : glycylglycine, 2; HEPES, 2; phthalate, 2; and CAPS, (2). $NaHCO_3$ was replaced with NaCl and the external solution was gased and mixed with 100% O_2. This Ringer was found, by acid titration, to have similar buffering capacities in the pH regions of 11 to 10, 8.5 to 6.8, and 5.5 to 4.0. The internal solution remained at pH 7.4 throughout the experiment. The pH of the external solution was adjusted with HCl. TAP stock solutions were adjusted to the appropriate pH before each addition. Figure 7 illustrates the inhibition (plotted as V') of I_{sc} caused by a submaximal dose of TAP (1.25 mM) as a function of external pH after the skin had equilibrated at each pH value for 15 to 20 min (closed circles ±SE). It was observed that TAP became more effective as the external pH was reduced.

To analyze which molecular form of TAP (neutral, mono-cation, or dication) is the active form, the following calculations were made while assuming that only one form of TAP is active. The theoretical K_I, defined as the concentration of each particular species that would be necessary to cause 50% inhibition of I_{sc}, was calculated for each TAP species from the Henderson-Hasselbalch equations at the pH (approx. 7.1) where $V' = 0.5$ (50% inhibition of I_{sc}). Theoretical curves for each species of TAP were subsequently computed for the V' *vs.* pH plot using these theoretical K_I's, species concentrations calculated from the Henderson-Hasselbalch equation, and V' obtained from the noncompetitive kinetic model discussed earlier (Eq. (5)). These theoretical curves are also plotted

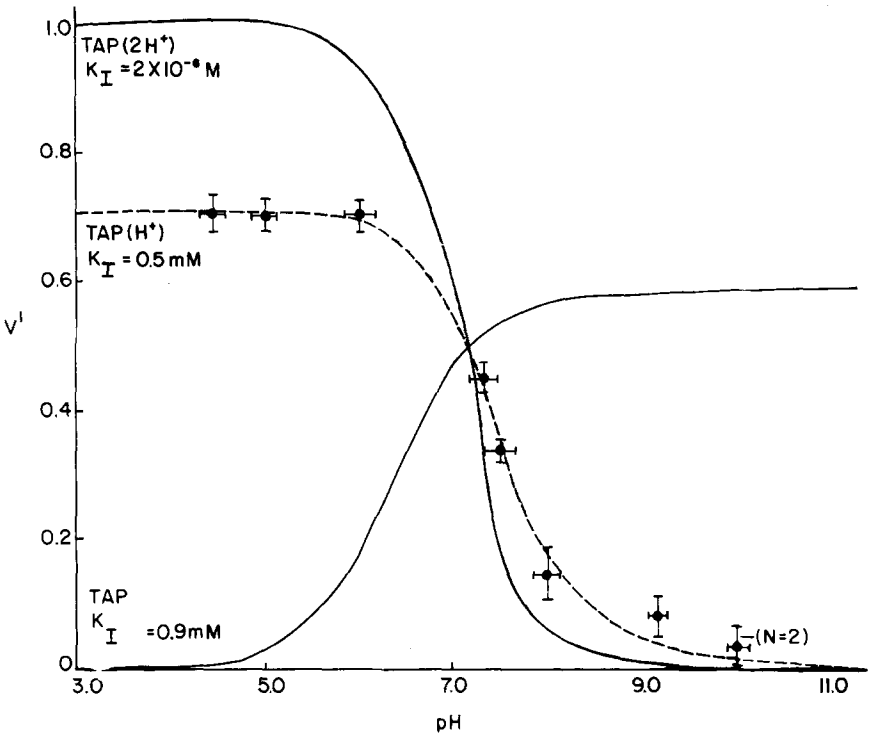

Fig. 7. Effect of external pH on the inhibitory potency of 1.25 mM TAP in the external solution of frog skin. Data are presented as the fractional inhibition (V') produced by 1.25 mM TAP *vs.* external pH. Experiments were performed in a specially buffered external medium containing (in mM): 2, glycylglycine; 2, HEPES; 2, phthalate; and 2, CAPS. Theoretical lines are plotted for each of the species of TAP using the inhibitory model described in the text and the Henderson-Hasselbalch equation. Data points represent the mean of 7 experiments, except at pH 10.2 where only 2 skins were successfully equilibrated. Bars indicate 1 SEM, except at pH 10.2 where they represent the range

in Fig. 7 and are appropriately labeled. It is clearly shown in Fig. 7, that the best fit for the experimental points is the mono-protonated form of TAP (dashed line).

C. Effect of External Ca

The effect of external Ca on TAP inhibition was studied since it has been shown that Ca noncompetitively inhibits Na transport from the external solution in frog skin (Mandel, 1978) and, in addition, Ca may be necessary for amiloride to effectively inhibit Na entry in some species of

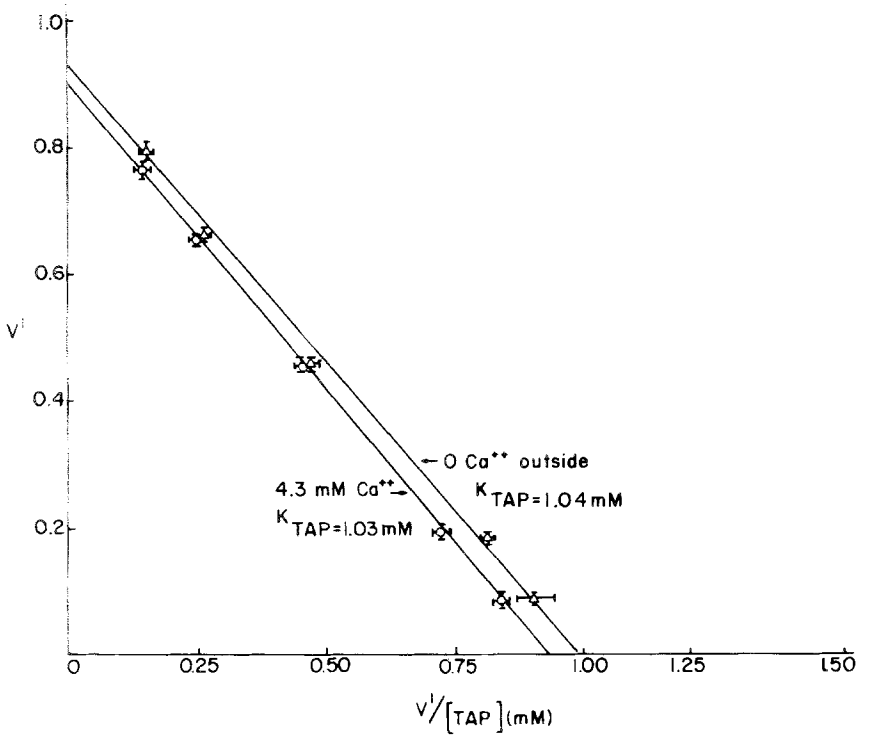

Fig. 8. Single reciprocal plot of V' *vs.* $V'/[\text{TAP}]$ in the presence and absence of 4.3 mM calcium in frog skin. Data points represent the mean of 6 experiments; bars indicate 1 SEM

frog skin (Cuthbert & Wong, 1972; Benos *et al.*, 1976). As Fig. 8 illustrates, the removal of Ca had no effect on the inhibitory action of TAP.

D. Interaction Between TAP and Amiloride

The results described above for TAP indicate that its inhibitory action has similar properties to those of amiloride in this preparation (Benos *et al.*, 1979). Thus, we decided to study the interaction between these two agents, the two simplest possibilities being: (i) TAP and amiloride bind to the same site and thus are mutually exclusive with each other, or (ii) TAP and amiloride bind to spacially distinct sites which do not interact. To investigate these possibilities, a kinetic model for the noncompetitive inhibition of I_{sc} by TAP and amiloride was formulated by first assuming that TAP and amiloride were mutually exclusive (*see Appendix*). From this model, a Dixon plot (*Appendix*, Eq. (A6)) of $1/I_{sc}$ *vs.* the concentration of TAP performed at different

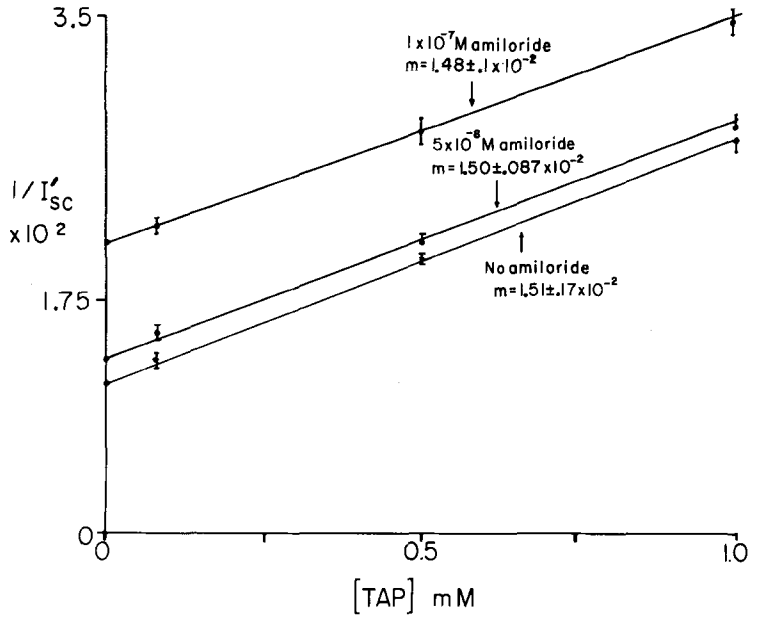

Fig. 9. Dixon plot of $1/I_{sc}$ *vs.* TAP concentration at 3 amiloride concentrations, 0, 5×10^{-8}, and 1×10^{-7} M. I'_{sc} represents the I_{sc} normalized to 100 at I_{max}. Data points represent the mean of 5 frog skins; bars indicate 1 SEM

amiloride concentrations should result in a family of parallel lines, with a slope equal to:

$$\frac{1+K_{Na}}{[Na]} \Big/ K_{TAP} I_{max}.$$

Conversely, if TAP and amiloride did not bind to the same site, the Dixon plot would result in a family of lines not parallel to each other which would intersect at the point whose coordinates would be given by K_{TAP} (abscissa-value) and $1/I_{max}(1+K_{Na}/[Na])$ (ordinate-value) (*see* Segel, 1975). Figure 9 illustrates that to concentrations of amiloride, 5×10^{-8} M and 1×10^{-7} M, resulted in parallel displacements of the TAP Dixon plots with the slope remaining constant at approximately 1.5×10^{-2}. This behavior is indicative of two mutually exclusive inhibitors which directly interact with each other, possibly binding to the same site.

Effect of Amiloride on the Tight Junctional Cation Conductance in Frog Gallbladder

Figure 10 shows a typical experiment in which the effects of amiloride were tested on the sodium conductance of the gallbladder. The spon-

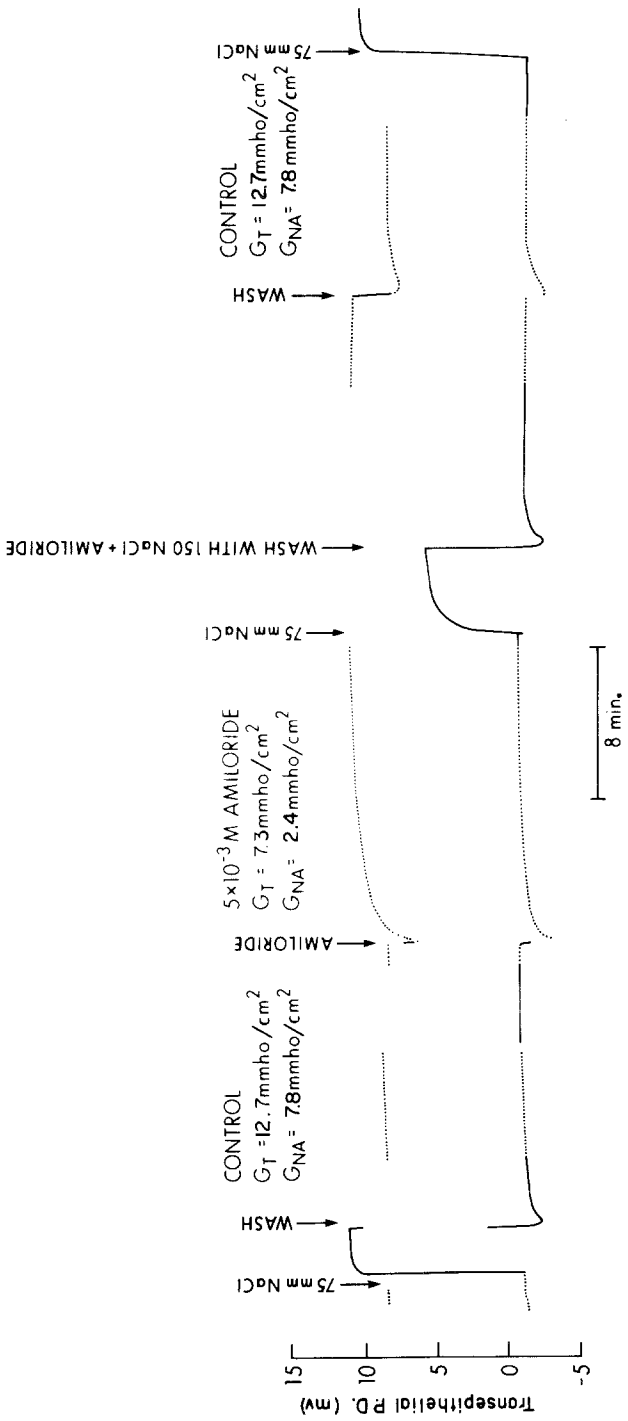

Fig. 10. Effect of 5×10^{-3} M amiloride on the total tissue conductance (G_T) and Na conductance (G_{Na}) of the frog gallbladder. Amiloride was added to both the mucosal and serosal solutions simultaneously; conductance was determined from the voltage deflection (upper points on tracing) in response to a transepithelial depolarizing pulse. NaCl dilution potentials were obtained by replacing the 150 mM NaCl solution with 75 mM NaCl at the times indicated

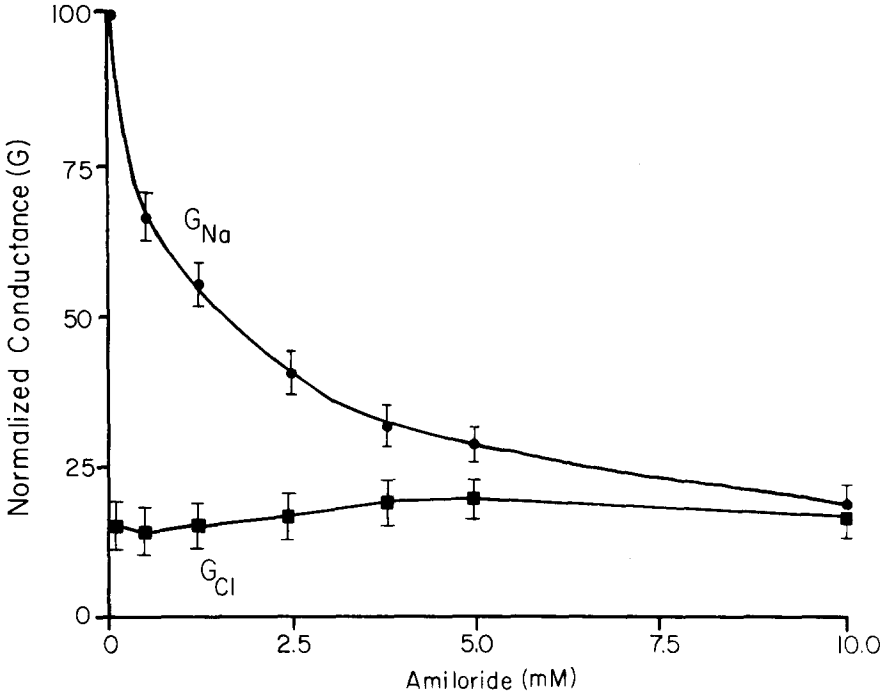

Fig. 11. Dose response of amiloride inhibition of G_{Na} and G_{Cl} in the frog gallbladder. Amiloride was added to both sides of the epithelium. Data are presented as conductances normalized to control G_{Na} (equal to 100), *vs.* the amiloride concentration. Data points represent the mean of 6 experiments; bars indicate 1 SEM

taneous PD of -2 mV is depicted by the bottom trace, whereas the top trace shows the deflection produced by a transepithelial current pulse; G_T was determined from the magnitude of this deflection, using Ohm's law. The dilution potential and G_T were measured prior to and after the addition of amiloride; G_{NA} was calculated as described in *Methods*. After 5 mM amiloride was added to both sides of the gallbladder, both G_T and the dilution potential decreased, resulting in a decrease in G_{Na}. In 6 bladders the mean decrease in G_T and G_{Na} was 43.4 ± 0.6 % and 69.2 ± 0.6 %, respectively. This effect is also completely reversible (Fig. 10). Amiloride was effective from either the mucosal or serosal solutions alone; however, the time course for serosal inhibition was much slower.

Figure 11 illustrates a dose response curve of amiloride on G_{Na} and G_{Cl} in 6 gallbladders. All conductance values were normalized to the control G_{Na}. No significant change in G_{Cl} was observed with increasing amiloride concentrations. In contrast, G_{Na} was strongly inhibited in a dose dependent manner. The apparent K_I for the amiloride inhibition was estimated to be 2 mM from this curve.

The interaction between amiloride and Na was further studied in an attempt to determine whether the inhibition was competitive or noncompetitive. To this end, the inhibition of G_{Na} by amiloride was measured as a function of Na concentration in the bathing media (isosmotic mannitol replacement). The interpretation of the results was complicated by the observation that the magnitude of the dilution potential was dependent on the absolute Na concentration. For example, the measured dilution potential was 12.2 ± 0.5 mV when the NaCl gradient applied across the gallbladder was 150 mM (serosal side)/75 mM (mucosal side), whereas this potential was 7.4 ± 0.8 mV when the NaCl gradient was 50/25 mM. Since the Goldman-Hodgkin-Katz equation predicts near identical dilution potentials (within 3 %) for these two situations, it appears that the absolute permeability of the gallbladder is dependent on the absolute NaCl concentration or ionic strength. A similar effect was observed for RbCl dilution potentials in gallbladder by Wright, Barry and Diamond (1971). The effect of low NaCl was completely reversible. Expressing the inhibition of G_{Na} by amiloride as a percent, it is found that 5 mM amiloride is equally effective in both a 150/75 mM NaCl gradient and a 50/25 mM gradient: 69.2 ± 0.6 and 67.8 ± 0.9 %, respectively, for 5 experiments. This behavior is indicative of a noncompetitive inhibition, i.e., 5 mM amiloride is equally effective at the lower Na concentrations. However, this result is not conclusive, due to the aforementioned changes in the permeability characteristics of the bladder by the reduced Na.

The mean values for 6 amiloride dose-response experiments were plotted in the single reciprocal form V' *vs.* V'/[amiloride] introduced earlier, to determine whether a simple Michaelis-Menten kinetic scheme (eq. (5)) describes the inhibition of G_{Na} by amiloride. Figure 12 illustrates that the amiloride interaction apparently does follow this kinetic scheme. The K_I of amiloride obtained from the slope of this line was 1.2 mM.

Amiloride only exists in two forms, protonated at low pH and unprotonated at high pH with a pK_a of 8.7. The influence of pH on the inhibition of G_{Na} by a 2 mM dose of amiloride was studied at three pH values: 4.5, 7.0, and 9.7 in order to investigate whether both or only one of these species is responsible for amiloride's inhibitory action. The standard gallbladder Ringer was supplemented in these studies with 2 mM phthalate and 2 mM CAPS to stabilize the pH at 4.5 and 9.7, respectively. The percent inhibition of G_{Na} by 2 mM amiloride was 54.6 ± 1.8 % at pH 4.5, 56.3 ± 1.3 % at pH 7.0, and 45.6 ± 2.1 % at pH 9.7 in four bladders. It should be noted that the inhibitory action of amiloride at pH 9.7 was only slightly lower than the inhibition observed at the

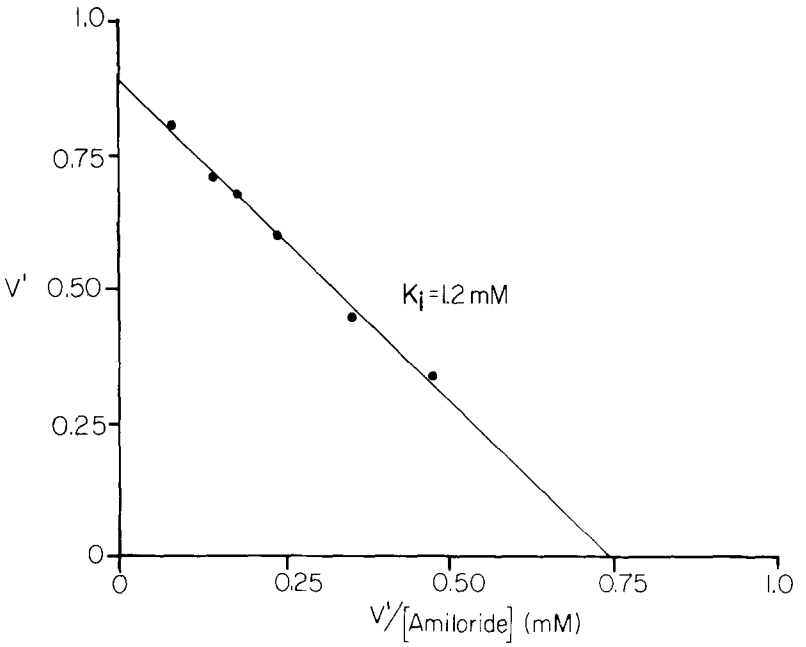

Fig. 12. Single reciprocal plot of the fractional inhibition of G_{Na} (V') in gallbladder produced by amiloride *vs.* V' divided by the amiloride concentration (V'/[amiloride]). Points represent the mean of 6 experiments. The regression line through the data points has a correlation coefficient of >0.99

lower pH's, despite the fact that at this pH the unprotonated form of amiloride predominates. The Henderson-Hasselbalch equation would predict that the protonated species of amiloride would be 0.18 mM in a 2 mM amiloride solution at pH 9.7. If the only active form were the protonated species, the kinetic model would predict that amiloride should inhibit only 10% of the G_{Na} at pH 9.7. These data indicate that both the unprotonated and the protonated species of amiloride inhibit the G_{Na} in the gallbladder, although the K_I of the unprotonated form may be somewhat higher than the protonated form.

Discussion

Previous investigators have demonstrated that TAP blocks the extracellular junctional cation permeation in leaky epithelia (Moreno, 1975) and that amiloride blocks the cellular cation permeation pathway in tight epithelia (Salako & Smith, 1970; Biber, 1971). In addition, Lewis

and Diamond (1976), Balaban and Mandel (1978), and Reuss and Grady (1979) have briefly described some effects of TAP on cellular cation pathways. This study provides evidence that both TAP and amiloride are able to inhibit either of these cation permeation pathways.

The inhibition of Na entry in frog skin by TAP exhibits numerous similarities to the inhibitory action of amiloride. These similarities are: (i) both inhibit rapidly and reversibly from the external solution (Fig. 1); (ii) both are noncompetitive with external Na in bullfrog (Fig. 4; also Benos *et al.*, 1979) and, therefore, TAP and amiloride appear to interact with a site spacially distinct from the Na-interaction site; (iii) neither TAP (Fig. 8) nor amiloride (Benos *et al.*, 1979) require the presence of external calcium to enhance their inhibitory activity in bullfrog skin; (iv) both drugs are only active in the monoprotonated form (Fig. 7; also Benos *et al.*, 1979); and (v) TAP and amiloride are mutually exclusive with each other in their inhibitory action (Fig. 9). All of these similarities suggest that TAP and amiloride may interact at the same inhibitory site. Various types of molecular interactions could elicit mutually exclusive behavior, the simplest model being that TAP and amiloride actually bind to the same site. More complex interactions would involve steric effects either at the same site or at spacially distinct sites which inactivate each other when either site is occupied. Evidence is presented later in this section which appears compatible with the simple single-site model.

Despite these similarities, several notable differences do exist between the TAP and amiloride inhibition of Na entry in frog skin: (i) a large difference in K_I exists between these two drugs; amiloride has a K_I of approximately 10^{-6} M in the bullfrog skin (Benos *et al.*, 1979) while the K_I of TAP was found to be approximately 10^{-3} M; (ii) amiloride interacts with its inhibitory site in a complex manner (Benos *et al.*, 1976; 1979), whereas TAP inhibition can be adequately described by a noncompetitive Michaelis-Menten kinetic model (Fig. 5). Furthermore, the calculated Hill coefficient of approximately 0.5 for amiloride indicates that negative cooperativity is present in its interaction with bullfrog skin (Benos *et al.*, 1979). In contrast, TAP was found to have a Hill coefficient of approximately 1.0 in this study, indicating that TAP interacts with its site in a one-to-one manner with little or no cooperativity. (iii) TAP's potency was a function of the external buffering capacity at pH 7.4 (Fig. 6) while amiloride's action was independent of this variable.

In the frog gallbladder, amiloride inhibited the cationic conductance of the extracellular junctional pathway with the following properties in common with TAP: (i) both inhibit rapidly and reversibly (Fig. 10; also

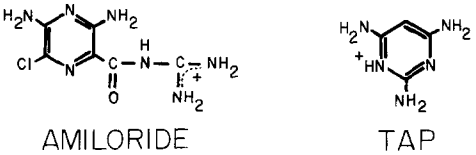

Fig. 13. Protonated species of TAP and amiloride

Moreno, 1975); (ii) both display similar K_I's of approximately 1 mM; (iii) the inhibitory action of both drugs may be described by a simple noncompetitive model (Fig. 12; also Moreno, 1975); and (iv) in both cases, the monoprotonated form of the drug is active, although an important difference in this category is the observed inhibitory activity of amiloride in the neutral form.

The nature of the TAP inhibitory site in the gallbladder has been analyzed in detail by Moreno (1975). Experiments performed in the gallbladder demonstrated that acid titration of the bathing medium inhibited cation permeation through the junctional pathway with an apparent pK_a of 4.5. Based on these results, Moreno postulated that the extracellular junctional permeation site is partially composed of acidic groups which, when titrated, abolish cation permeation (Moreno & Diamond, 1975*a*). Using this hypothesis, Moreno (1975) proposed a mechanism in which TAP inhibits the junctional pathway by associating with these acidic groups through the formation of a double hydrogen bond between two partially negatively charged oxygens in either carboxyl or phosphate groups. This bonding conformation of TAP has also been proposed by Roth and Strelitz (1969) due to the anomalous behavior of TAP in dilute phosphate solutions.

Amiloride possesses a pyrazine ring which has a very similar structure and hydrogen bonding capability as the mono-protonated form of TAP, due to the electron-widthdrawing Cl located at the 6-ring position and amino groups at the 3 and 5 positions (*see* Fig. 13 for comparison). These hydrogen bonding amino groups could also form the double hydrogen bond with carboxyl and/or phosphate groups as has been proposed by Moreno (1975) for the TAP molecule. Thus, it is possible that amiloride and TAP both react at related types of sites in gallbladder by virtue of these similar properties. Support for the notion that the pyrazine ring in amiloride is responsible for its inhibitory activity in gallbladder comes from the present results which demonstrate that amiloride is active in the unprotonated form. The charge in amiloride is located in the acyl-guanidinium group (Benos *et al.*, 1976) and, thus, it

would appear that this portion of the molecule would be less important for the junctional pathway inhibition. It should be noted that the charge on the TAP molecule is necessary to potentiate this proposed hydrogen bonding scheme, since TAP does not contain an electron withdrawing group on its ring. Thus, electrostatic interactions by the charge *per se* may not be involved in the inhibitory action of TAP.

The high affinity and complex interaction of amiloride with the cellular entry site may be in part the result of properties of each component of the molecule. The inhibitory activity of amiloride is highly dependent on the integrity of the pyrazine ring with most of its substituents intact, including the acyl-guanidinium group located at position 2 in the ring which must be in the protonated (charged) form (Benos *et al.*, 1976). Therefore, in a simplified way, the interaction of amiloride with its site may be visualized as consisting of two partial interactions, one with the pyrazine ring and the other with the charged acyl-guanidinium. Since the kinetic studies (Fig. 8) indicate that TAP and amiloride may indeed vie for the same inhibitory sites in frog skin, it might be possible to learn something about the amiloride interaction with its site from the properties described earlier for TAP. The inhibitory action of TAP is essentially identical in gallbladder as in frog skin: (i) the same K_I in both tissues, (ii) the same active species in both preparations, and (iii) the kinetics of TAP inhibition in both systems obey Michaelis-Menten kinetic models. These results suggest that the junctional pathway in gallbladder and the cellular entry pathway in frog skin may possess certain comparable pharmacological properties. The ability to hydrogen bond appears to be important for the action of TAP in gallbladder, and this may also account for its action on frog skin. It has been shown that acid titration of the skin also abolishes Na permeation (Schoeffeniels, 1955; Mandel, 1978) and, more directly, recent experiments suggest that carboxyl and/or hydroxyl groups may be located at the amiloride binding site in frog skin (Mandel, Benos & Simon, 1978). Similarly, hydrogen bonding may also be an essential property of amiloride in frog skin, obtainable through its substituted pyrazine ring structure. The high affinity of amiloride would then be a function of the additional interaction with the charged acyl-guanidinium group. This model, however, is not unique and other possibilites need to be considered; for example, it is possible that TAP binds to the same site as the acyl-guanidinium group in amiloride and the high affinity of amiloride is obtained from the added interaction with the pyrazine ring.

Experiments with different buffers and buffering capacity demonstrated that the potency of TAP was dependent on the buffering capacity of the outer solution (Fig. 6). It is unlikely that this effect was the result of the buffer itself since several unrelated buffers (HEPES, Tris, and bicarbonate) had similar effects. The simplest explanation for this observed effect of buffer capacity on the inhibitory action of TAP may be that the presence of buffers caused changes in the local pH at the TAP inhibitory site. TAP is most effective in the acidic, monoprotonated form with a pK_a of 7.1 (Fig. 7). Since the pH in these experiments was 7.4, the charge and hence the potency of the TAP molecule would be greatly affected by small changes in pH at its inhibitory site. TAP would become more potent with slight acidifications and less potent with a slight alkalinization. Therefore, we speculate that with a low buffering capacity the pH at the inhibitory site may be more alkaline than the bulk solution, resulting in a low TAP potency. As the buffering capacity of the medium increased, the pH of this site would decrease toward the pH of the bulk solution, resulting in increased TAP potency. If this interpretation is correct, the TAP site is unlikely to be located at the exterior of the apical membrane of this epithelium since the skin was observed to acidify the external solution when this solution had a low buffering capacity. The unstirrred layer at the outer membrane would be predictably more acidic than the bulk solution due to this acid extrusion process. A more likely position for this site would be some location within the membrane where both the intracellular and extracellular pH and buffering capacities would influence its pH. In the low buffering capacity situation, the intramembrane pH may be governed more by the intracellular pH which may be significantly alkaline in relation to the extracellular space due to the acid extrusion at the outer barrier.

No effect of buffering capacity on amiloride inhibition of I_{sc} was found in these studies, even though the kinetic data and a comparison of the structures of TAP and amiloride suggest they may bind to the same inhibitory site. This result is probably due to the relatively high amiloride pK_a of 8.7, which is distinctly different from pH 7.4 used in these studies. Thus, the charge on amiloride, and therefore its potency would not be greatly affected by small changes in pH within this range. This latter result also suggests that the affinity of the binding site for TAP and amiloride is not affected by the buffers and, therefore, the observed changes in K_{TAP} occurring with alterations of buffering capacity are most likely an effect on the TAP molecule itself (i.e., concentration of charged species) and not on its inhibitory site. This interpretation is supported by

the observation that TAP potency was independent of buffering capacity at pH 6.0, which is far removed from the TAP pK_a.

Further evidence that changes in buffering capacity may alter the intramembrane pH at the Na entry pathway is obtained from the results of the experiments which measured the effects of HCO_3 concentration on K_{Na} and I_{max}. Although a dependence of the active Na transport rate on HCO_3 concentration has been demonstrated in other epithelia (Chen & Walser, 1977; Green & Giebisch, 1975), the direction of this relationship is usually to increase active transport as the HCO_3 concentration increases, whereas the opposite is observed in this study. The simplest explanation for our results is that the buffering system 25 mM HCO_3/5 % CO_2 causes a decrease in the intramembrane or cytoplasmic pH as compared to 2.5 mM $NaHCO_3/CO_2$ even if both result in a bulk solution pH of 7.4. This notion is reasonable since CO_2 is highly permeant in the frog skin (Smith, Hughes & Huf, 1971) and, therefore, the intramembrane and possibly cytoplasmic pH would be decreased by the increased CO_2 concentration. The decrease in I_{sc} obtained in Table 1 is comparable to that measured by Mandel (1978) when the cytoplasmic pH was decreased. In that study, the author presented evidence that the effects of intramembrane or cytoplasmic pH on I_{sc} occur by inhibiting the rate of Na permeation through the entry pathway noncompetitively. The present results are comparable in that the inhibition of I_{sc} by HCO_3/CO_2 was noncompetitive with Na. Other buffers, such as HEPES, were found not to inhibit the I_{sc} with increasing concentration. However, as with the HCO_3/CO_2 buffer, increasing the HEPES concentration did augment the potency of TAP. This result can be explained by the relative effectiveness of HCO_3/CO_2 and HEPES in buffering the intramembrane or cytoplasmic pH. HEPES is a large organic buffer which may not be as effective as HCO_3/CO_2 in buffering the intramembrane or cytoplasmic pH. Thus, with HEPES, the pH in this region may only shift sufficiently to change the potency of TAP but not enough to titrate the proton inhibitory site.

In conclusion, it is evident that TAP and amiloride both have capabilities of blocking each of the passive cation permeation pathways found in these epithelia. This result has allowed us to define certain pharmacological and kinetic similarities between these two pathways and assist in the elucidation of the chemical nature and molecular localization of their interactive sites. In addition, the cross-reactivity of these drugs emphasizes that care need be taken in the use of these drugs as "specific" agents in modifying epithelial transport functions.

It is a pleasure to acknowledge the excellent technical aid of Kathie Collatos. This work was supported by National Institutes of Health Grants AM-16024, GM-00929, and AM-05624.

Appendix

Derivation of the Equation for the Noncompetitive, Mutually Exclusive Simultaneous Inhibition of I_{sc} by Amiloride and TAP

For this analysis we assume, as discussed earlier, that the interaction of Na, TAP, and amiloride may be treated by Michaelis-Menten kinetics. TAP inhibition was shown in this study to follow a simple noncompetitive model which has been derived elsewhere (*see* Segel, 1975) and is illustrated in Eq. (A1).

$$I_{TAP}=\frac{I_{max}[Na]}{([Na]+K_{Na})\left(1+\frac{[TAP]}{K_{TAP}}\right)} \tag{A1}$$

where I_{TAP} is the I_{sc} at a particular TAP concentration. All the other terms have been defined in the text. Since $I_{sc}=I_{max}[Na]/([Na]+K_{Na})$, dividing both sides of Eq. (A1) by I_{sc} (the current observed in the absence of TAP), we obtain:

$$\frac{I_{TAP}}{I_{sc}}=\frac{1}{1+[TAP]/K_{TAP}}. \tag{A2}$$

Utilizing the expression for fractional inhibition $V'=1-I_{TAP}/I_{sc}$ defined in Eq. (4) and rearranged, we obtain:

$$V'=1-\frac{V'K_{TAP}}{[TAP]} \tag{A3}$$

which is Eq. (5) of the text.

Amiloride, however, does not obey a simple noncompetitive model, but was previously shown to obey the modified model depicted in Eq. (A4) (Benos *et al.*, 1979)

$$I_{Am}=\frac{I_{max}[Na]}{([Na]+K_{Na})\left(1+\left(\frac{[A]}{K_{Am}}\right)^{0.5}\right)} \tag{A4}$$

where I_{Am} is the I_{sc} at a particular amiloride concentration, [A] is the amiloride concentration and K_{Am} is the apparent amiloride Michaelis-Menten affinity constant.

Combining these two models with the condition that TAP and amiloride are mutually exclusive results in the following equation:

$$I_{sc} = \frac{I_{max}[Na]}{K_{Na}\left(1+\left(\frac{[A]}{K_{Am}}\right)^{0.5}+\frac{[TAP]}{K_{TAP}}\right)+[Na]\left(1+\left(\frac{[A]}{K_{Am}}\right)^{0.5}+\frac{[TAP]}{K_{TAP}}\right)}. \tag{A5}$$

For an in depth discussion of this type of derivation, *see* Segel (1975).

The mutual exclusivity of TAP and amiloride will be evident from the Dixon plots of $1/I_{sc}$ *vs.* the concentration of TAP at fixed [Na] and various fixed concentrations of amiloride. The equation for the Dixon plot is:

$$1/I_{sc} = \frac{1+\frac{K_{Na}}{[Na]}}{K_{TAP}I_{max}}[TAP]+\frac{1}{I_{max}}\left(1+\frac{K_{Na}}{[Na]}+\left(\frac{[A]}{K_{Am}}\right)^{0.5}+\frac{K_{Na}}{[Na]}\left(\frac{[A]}{K_{Am}}\right)^{0.5}\right) \tag{A6}$$

From Eq. (A6), it is evident that the slope of these Dixon plots should be independent of the amiloride concentration, while the intercept of the $1/I_{sc}$ axis represents the effect of varying concentrations of amiloride in the absence of TAP.

Plotting experimental data in a Dixon plot (Fig. 9) resulted in straight lines ($r^2 > 0.99$) which agreed with this model on several points. First, the constant slope of the plots was experimentally determined to be $1.51 \pm 0.17 \times 10^{-2}$. Using Eq. (A6), the theoretical slope is 1.48×10^{-2} using a K_{Na} of 18 mM (Benos *et al.*, 1979), [Na] of 110 mM and K_{TAP} = 0.8 mM. Secondly, the $1/I_{sc}$ intercept in the presence of 1×10^{-7} M amiloride was found to be $1.98 \pm 0.14 \times 10^{-2}$, while the calculated $1/I_{sc}$ intercept was 1.99×10^{-2} with a [A] of 10^{-7} M, K_{Am} of 2×10^{-7} M, K_{Na} of 18 mM and [Na] of 110 mM. Finally, amiloride shifts the Dixon plot in the predicted manner (i.e., parallel shift). If TAP and amiloride were nonmutually exclusive or cooperative, the slope of the Dixon plot would increase with increasing amiloride concentration (Segel, 1975).

References

Balaban, R.S., Mandel, L.J. 1978. 2,4,6 Triaminopyrimidine (TAP) inhibition of active Na transport in frog skin. *Biophys. J.* **21**:151*a*

Barry, H.B., Diamond, J.M. 1970. Junction potentials, electrode standard potentials, and other problems in interpreting electrical properties of membranes. *J. Membrane Biol.* **3**:93

Barry, P.H., Diamond, J.M. 1971. A theory of ion permeation through membranes with fixed neutral sites. *J. Membrane Biol.* **4**:295

Barry, P.H., Diamond, J.M., Wright, E.M. 1971. The mechanism of cation permeation in rabbit gallbladder. Dilution potentials and biionic potentials. *J. Membrane Biol.* **4**:358

Benos, D.J., Mandel, L.J., Balaban, R.S. 1979. On the mechanism of the amiloride-sodium entry site interaction in anuran skin epithelia. *J. Gen. Physiol.* **73**:307

Benos, D.J., Simon, S.A., Mandel, L.J., Cala, P.M. 1976. Effect of amiloride and some of its analogues on cation transport in isolated frog skin and thin lipid membranes. *J. Gen. Physiol.* **68**:43

Biber, T.U.L. 1971. Effect of changes in transepithelial transport on the uptake of sodium across the outer surface of the frog skin. *J. Gen. Physiol.* **58**:131

Cala, P.M., Cogswell, N., Mandel, L.J. 1978. Binding of [H^3] ouabain to split frog skin. The role of Na, K-ATPase in the generation of short circuit current. *J. Gen. Physiol.* **71**:347

Chen, J.S., Walser, M. 1977. Bicarbonate ions in active sodium transport across toad bladder. *Am. J. Physiol.* **231**:F210

Cuthbert, A.W. 1977. Aspects of the pharmacology of passive ion transfer across cell membranes. *Prog. Med. Chem.* **14**:1

Cuthbert, A.W., Shum, W.K. 1976. Characteristics of the entry process for sodium in transporting epithelia as revealed with amiloride. *J. Physiol. (London)* **255**:587

Cuthbert, A.W., Wong, P.Y.D. 1972. The role of calcium ions in the interaction of amiloride with membrane receptors. *Mol. Pharmacol.* **8**:222

Diamond, J.M. 1978. Channels in epithelial cell membranes and junctions. *Fed. Proc.* **37**:2639

Fromter, E., Diamond, J.M. 1972. Route of passive permeation in epithelia. *Nature New Biol.* **235**:9

Green, R., Giebisch, G. 1975. Ionic requirements of proximal sodium transport. I. Bicarbonate and chloride. *Am. J. Physiol.* **229**:1205

Helman, S.I., Fisher, R.S. 1977. Microelectrode studies of the active Na transport pathway of frog skin. *J. Gen. Physiol.* **69**:571

Lewis, S.A., Diamond, J.M. 1976. Na^+ transport by rabbit urinary bladder, a tight epithelium. *J. Membrane Biol.* **28**:1

Lindemann, B., Voute, C. 1976. Structure and function of the epidermis. *In:* Frog Neurobiology. R. Llinas and W. Precht, editors. Springer-Verlag, Berlin

Mandel, L.J. 1978. Effects of pH, Ca, ADH, and theophylline on the kinetics of Na entry in frog skin. *Am. J. Physiol.* **35**: *C* 35

Mandel, L.J., Benos, D.J., Simon, S.A. 1978. Chemical probing of the Na-entry mechanism in frog skin epithelium with site-specific reagents. Sixth International Biophysics Congress, Kyoto, Japan

Mandel, L.J., Curran, P.F. 1973. Response of the frog skin to steady-state voltage clamping. II. The active pathway. *J. Gen. Physiol* **62**:1

Moreno, J.H. 1975. Blockage of gallbladder tight junction cation-selective channels by 2-4-6 triaminopyrimidinium (TAP). *J. Gen. Physiol.* **66**:97

Moreno, J.H., Diamond, J.M. 1974. Discrimination of monovalent cations by "tight" junctions of gallbladder epithelium. *J. Membrane Biol.* **15**:277

Moreno, J.H., Diamond, J.M. 1975*a*. Cation permeation mechanisms and cation selectivity in "tight junctions" of gallbladder. *In:* Membranes—A Series of Advances. G. Eisenman, editor. Vol. 3, p. 383. Marcel Dekker, New York

Moreno, J.H., Diamond, J.M. 1975*b*. Nitrogenous cations as probes of permeation channels. *J. Membrane Biol.* **21**:197

Reuss, L., Grady, T.P. 1979. Effects of triaminopyrimidine on electrical pathways of gallbladder epithelium. *Biophys. J.* **25**:31*a*

Robinson, R.A., Stokes, R.H. 1970. Electrolyte Solutions. Butterworth & Co., London

Roth, B., Strelitz, J.Z. 1969. The protonation of 2,4-diaminopyrimidines I. Dissociation constants and substituent effect. *J. Org. Chem.* **34**:821

Salako, L.A., Smith, A.J. 1970. Changes in sodium pool and kinetics of sodium transport in frog skin produced by amiloride. *Br. J. Pharmacol.* **39**:99

Schoeffeniels, E. 1955. Influence du pH sur le transport actif de sodium a travers la peau de grenoulille. *Arch. Int. Physiol. Biochim.* **63**:513

Schultz, S.G., Zalusky, R. 1964. Ion transport in isolated rabbit ileum. I. Short-circuit current and Na fluxes. *J. Gen. Physiol.* **47**:567

Segel, I.H. 1975. Enzyme Kinetics, John Wiley & Sons, New York

Smith, T.C., Hughes, W.D., Huf, E.G. 1971. Movement of CO_2 and HCO_3 across isolated frog skin. *Biochim. Biophys. Acta* **225**:77

Ussing, H.H., Zerahn, K. 1951. Active Transport of sodium as the source of electric current in the short-circuited isolated frog skin. *Acta Physiol. Scand.* **36**:110

Wright, E.M., Barry, P.H., Diamond, J.M. 1971. The mechanism of cation permeation in rabbit gallbladder. Conductances, the current-voltage relation, the concentration dependence of anion-cation discrimination, and the calcium competition effect. *J. Membrane Biol.* **4**:331